MEDICAL SCIENCE MONITOR

CLINICAL RESEARCH

e-ISSN 1643-3750
© Med Sci Monit, 2021; 27: e933959
DOI: 10.12659/MSM.933959

Received: 2021.07.11
Accepted: 2021.08.10
Available online: 2021.08.19
Published: 2021.10.17

White Matter Abnormalities in Traumatic Subarachnoid Hemorrhage: A Tract-Based Spatial Statistics Study

Authors' Contribution:
Study Design A
Data Collection B
Statistical Analysis C
Data Interpretation D
Manuscript Preparation E
Literature Search F
Funds Collection G

ABCDE 1 Min Son Kim
CDE 1 Min Jye Cho*
CDF 2 Jae Woon Kim
AEF 1 Sung Ho Jang*

1 Department of Physical Medicine and Rehabilitation, College of Medicine, Yeungnam University, Namku, Taegu, South Korea
2 Department of Radiology, College of Medicine, Yeungnam University, Namku, Taegu, South Korea

* Min Jye Cho and Sung Ho Jang contributed equally to this work

Corresponding Author: Sung Ho Jang, e-mail: strokerehab@hanmail.net
Financial support: This work was supported by a National Research Foundation of Korea (NRF) grant funded by the Korean government (MSIP) (No. 2021R1A2B5B01001386)

Conflict of interest: None declared

Background: The pathophysiology of traumatic subarachnoid hemorrhage and brain injury has not been fully elucidated. In this study, we examined abnormalities of white matter in isolated traumatic subarachnoid hemorrhage patients by applying tract-based spatial statistics.

Material/Methods: For this study, 10 isolated traumatic subarachnoid hemorrhage patients and 10 age- and sex-matched healthy control subjects were recruited. Fractional anisotropy data voxel-wise statistical analyses were conducted through the tract-based spatial statistics as implemented in the FMRIB Software Library. Depending on the intersection between the fractional anisotropy skeleton and the probabilistic white matter atlases of Johns Hopkins University, we calculated mean fractional anisotropy values within the entire tract skeleton and 48 regions of interest.

Results: The fractional anisotropy values for 19 of 48 regions of interest showed significant divergences ($P<0.05$) between the patient group and control group. The regions showing significant differences included the corpus callosum and its adjacent neural structures, the brainstem and its adjacent neural structures, and the subcortical white matter that passes the long neural tract.

Conclusions: The results demonstrated abnormalities of white matter in traumatic subarachnoid hemorrhage patients, and the abnormality locations are compatible with areas that are vulnerable to diffuse axonal injury. Based on these results, traumatic subarachnoid hemorrhage patients also exhibit diffuse axonal injuries; thus, traumatic subarachnoid hemorrhage could be an indicator of the presence of severe brain injuries associated with acute or excessive mechanical forces.

Keywords: Anisotropy • Diffusion Tensor Imaging • Spatial Analysis • Subarachnoid Hemorrhage, Traumatic

Full-text PDF: https://www.medscimonit.com/abstract/index/idArt/933959

Indexed in: [Current Contents/Clinical Medicine] [SCI Expanded] [ISI Alerting System] [ISI Journals Master List] [Index Medicus/MEDLINE] [EMBASE/Excerpta Medica] [Chemical Abstracts/CAS]

Background

Subarachnoid hemorrhage (SAH) results in an accumulation of blood in the subarachnoid space and is mainly a sequela of head trauma [1]. Traumatic SAH occurs in 26-53% of traumatic brain injuries patients [2]. Previous studies have reported that traumatic SAH patients, either alone or with other brain injuries, have a poor outcome [3-7]. As a result, it has been argued that traumatic SAH can be an indicator of the presence of severe traumatic brain injuries. Among SAH-related secondary brain damages, post-traumatic vasospasm, hypothalamic-pituitary axis dysfunction, and hydrocephalus have been suggested as causes of the poor outcome in SAH patients [8-14]. However, the pathophysiology of traumatic SAH for brain injury has not been fully elucidated. Many studies have reported that traumatic brain injuries in most patients are accompanied by focal axonal injury or diffuse axonal injury (DAI) [15-23]. As SAH may be accompanied by axonal injuries, we hypothesized that traumatic SAH would be accompanied by traumatic axonal injuries.

Diffusion tensor imaging (DTI) allows the assessment of the white matter integrity because of imaging capability of water diffusion properties [24-26]. Specifically, tract-based spatial statistics (TBSS) derived from DTI is a delicate technique that conducts precise voxel-based white matter analysis and is suitable for implementation in multi-subject diffusion imaging-based studies [27]. In addition, TBSS avoids non-objective choice of regions of interest within hypothesis-based white matter areas [27]. Therefore, TBSS can provide comprehensive information on overall variations in the white matter's microstructure of the brain [27]. By using TBSS, several studies have demonstrated white matter changes in traumatic brain injuries; however, no study has reported abnormalities of white matter in isolated traumatic SAH patients [28-35].

In this study, we applied TBSS to investigate white matter abnormalities in patients with traumatic SAH.

Material and Methods

Subjects

Ten patients (6 men, 4 women; mean age 50.60±19.17 years; range, 23-79 years) were recruited according to the following inclusion criteria: (1) age: 20-80 years; (2) no history of previous head trauma or neurologic or psychiatric disease; (3) SAH due to head trauma, but no other definite brain lesion in the brain parenchyma (such as intracranial hemorrhage, intraventricular hemorrhage, hydrocephalus, or subdural hygroma), which was confirmed by a neuroradiologist; and (4) DTI data obtained after 4 weeks from hemorrhage onset. Ten age- and sex-matched healthy control subjects without previous history of psychiatric or neurologic disease or head trauma (6 men, 4 women; mean age 49.50±16.99 years, range 22-74 years) were also recruited as a control group. The demographic characteristics for the patient and control groups are listed in **Table 1**. Age or sex distribution identified no significant difference between the patient and control groups ($P>0.05$). This retrospective study was conducted following the requirements of the Declaration of Helsinki research guidelines and the recommendations of the Institutional Review Board of Yeungnam University Hospital. Signed informed consent was obtained from all of the subjects, and the study protocol was approved by the Institutional Review Board of Yeungnam University hospital (ethics approval number: YUMC-2021-03-014). In the case of patients with cognitive disorder or visual problem due to traumatic SAH, informed consent was provided through the caregiver.

Diffusion Tensor Imaging

DTI data were obtained at an average of 12.43±12.36 months after SAH onset by using a 1.5 T Philips Gyroscan Intera device (Hoffman-LaRoche, Best, Netherlands) with 32 non-collinear diffusion-sensitizing gradients by performing single-shot echo-planar imaging. For the 32 non-collinear diffusion-sensitizing gradients, 65 consecutive slices were obtained parallel to the anterior commissure – posterior commissure line [36]. Imaging parameters were as follows: acquisition matrix=96×96, reconstructed to matrix=192×192 matrix, field of view=240×240 mm, repetition time=10,398 ms, echo time=72 ms, echo-planning imaging factor=59 and b=1000 s/mm^2, slice gap=0, and slice thickness=2.5 mm [36]. Analysis of diffusion-weighted imaging data was conducted through the Oxford Centre for Functional Magnetic Resonance Imaging of the Brain (FMRIB) Software Library (www.fmrib.ox.ac.uk/fsl). The head motion effects and image distortion were corrected by utilizing affine multi-scale two-dimensional registration [37].

Tract-Based Spatial Statistics

All data analyses were conducted utilizing the functional MRI evaluation tool through the FMRIB software library (FSL) [38]. Fractional anisotropy (FA) maps were created using a previously described method [27]. Using TBSS realized in the FSL, voxel-wise statistical analysis of the FA data was conducted [39]. To sort the FA data for all subjects into a common space, a non-linear registration algorithm (www.doc.ic.ac.uk/~dr/software) was utilized [38]. A mean FA image was generated and then thinned to make a mean FA skeleton showing the centroids of all areas common to the group subjects [38]. We then applied a threshold to and binarized the mean FA skeleton at an FA level >0.2, and the adjusted data were entered into the voxel-wise statistics process. Then, for each subject, the sorted FA data were reflected to the mean skeleton, and to assess the

Indexed in: [Current Contents/Clinical Medicine] [SCI Expanded] [ISI Alerting System] [ISI Journals Master List] [Index Medicus/MEDLINE] [EMBASE/Excerpta Medica] [Chemical Abstracts/CAS]

Table 1. Demographic characteristics for the patient and control groups.

	Patient group (n=10)	Control group (n=10)
Age (years)	50.60±19.17	49.50±16.99
Sex (Male: Female)	6: 4	6: 4
Time to DTI scanning after onset (months)	12.43±12.36	NA
Loss of consciousness (*n* [%])		
<30 min	1 [0.1]	NA
30 min-24 h	4 [0.4]	NA
>24 hr	5 [0.5]	NA
Post-traumatic amnesia (*n* [%])		
<1 day	2 [0.2]	NA
1-7days	2 [0.2]	NA
>7 days	6 [0.6]	NA
Initial GCS score (*n* [%])		
13-15	1 [0.1]	NA
9-12	2 [0.2]	NA
3-8	7 [0.7]	NA
Traumatic brain injury (*n* [%])		
Mild	1 [0.1]	NA
Moderate	2 [0.2]	NA
Severe	7 [0.7]	NA
Cause (*n* [%])		
Passenger TA	1 [0.1]	NA
Pedestrian TA	3 [0.3]	NA
Slip/fall	4 [0.4]	NA
Bicycle	2 [0.2]	NA

Values represent mean±standard deviation; DTI – diffusion tensor imaging; NA – not applicable; GCS – Glasgow Coma Scale; TA – traffic accident.

FA values' differences between each group, voxel-wise cross-subject statistics were acquired [38]. The results were adjusted to control the family-wise error rate to allow multiple comparisons after conducting threshold-free cluster enhancement [38]. To confirm the mean FA values of each subject and observe the differences for each tract, voxels recognized as TBSS were chosen. We assessed mean FA values within the skeleton and 48 regions of interest (ROIs) that were depending on crossing between the entire skeleton and the probabilistic white matter atlases of Johns Hopkins University for organizing the FA data in each of the white matter regions [38]. Differences in the FA values among the 48 ROIs were determined by subtracting the average FA value of the patient group from that of the control group. The obtained FA values' differences were then arranged in descending order.

Statistical Analysis

Statistical analysis of the results was conducted using SPSS 21.0 for Windows (SPSS, Chicago, IL, USA). The chi-squared test was used to assess differences in the sex composition of the groups. The independent *t* test was performed to evaluate intergroup age differences and to examine the significance of FA values' differences between the patient and control groups. Statistical significance was considered for *P* values <0.05.

Results

The voxel-wise FA values' differences between the patient and control groups are listed in **Table 2** and, all of the ROIs are presented in ascending order, beginning with the ROI with

Indexed in: [Current Contents/Clinical Medicine] [SCI Expanded] [ISI Alerting System] [ISI Journals Master List] [Index Medicus/MEDLINE] [EMBASE/Excerpta Medica] [Chemical Abstracts/CAS]

Table 2. Results from the region of interest-based analysis of fractional anisotropy values of the patient and control groups.

	Patient group	Control group	Difference	p-Value
Splenium of corpus callosum	0.62±0.03	0.66±0.02	0.04	0.002*
Right posterior limb of internal capsule	0.55±0.02	0.58±0.01	0.03	0.003*
Right corticospinal tract	0.41±0.03	0.45±0.03	0.04	0.004*
Left cerebral peduncle	0.56±0.04	0.60±0.02	0.04	0.007*
Left superior corona radiata	0.40±0.02	0.44±0.02	0.04	0.008*
Right superior corona radiata	0.40±0.02	0.43±0.02	0.03	0.016*
Right posterior corona radiata	0.40±0.02	0.42±0.02	0.02	0.016*
Genu of corpus callosum	0.48±0.03	0.51±0.02	0.03	0.019*
Left corticospinal tract	0.41±0.05	0.46±0.03	0.05	0.023*
Left posterior limb of internal capsule	0.56±0.02	0.59±0.01	0.03	0.023*
Body of corpus callosum	0.51±0.03	0.56±0.04	0.05	0.028*
Right cingulum (hippocampus)	0.31±0.04	0.35±0.04	0.04	0.028*
Left anterior limb of internal capsule	0.45±0.03	0.48±0.02	0.03	0.028*
Middle cerebellar peduncle	0.42±0.02	0.44±0.02	0.02	0.028*
Left external capsule	0.35±0.02	0.37±0.02	0.02	0.028*
Left superior longitudinal fasciculus	0.40±0.02	0.42±0.01	0.02	0.034*
Left superior cerebellar peduncle	0.45±0.05	0.50±0.03	0.05	0.041*
Right superior cerebellar peduncle	0.147±0.06	0.52±0.03	0.05	0.041*
Left cingulum (cingulate gyrus)	0.43±0.03	0.46±0.02	0.03	0.049*
Right cerebral peduncle	0.56±0.03	0.59±0.02	0.03	0.059
Left posterior corona radiata	0.39±0.02	0.41±0.02	0.02	0.059
Left anterior corona radiata	0.35±0.04	0.39±0.03	0.04	0.070
Pontine crossing tract	0.39±0.03	0.42±0.02	0.03	0.070
Right anterior limb of internal capsule	0.46±0.02	0.48±0.02	0.02	0.070
Right superior fronto-occipital fasciculus	0.37±0.05	0.41±0.06	0.04	0.096
Left uncinate fasciculus	0.40±0.04	0.42±0.02	0.02	0.096
Right tapetum	0.33±0.03	0.35±0.04	0.02	0.096
Left superior fronto-occipital fasciculus	0.35±0.04	0.40±0.07	0.05	0.112
Right anterior corona radiata	0.35±0.03	0.38±0.03	0.03	0.112
Left cingulum (hippocampus)	0.32±0.04	0.35±0.03	0.03	0.131
Left fornix (crus)	0.42±0.04	0.45±0.04	0.03	0.131
Right external capsule	0.34±0.02	0.36±0.02	0.02	0.131
Right cingulum (cingulate gyrus)	0.40±0.03	0.42±0.02	0.02	0.131
Right medial lemniscus	0.52±0.03	0.54±0.02	0.02	0.151
Left sagittal stratum (include inferior longitudinal fasciculus and inferior fronto-occipital fasciculus)	0.42±0.02	0.44±0.03	0.02	0.151

Indexed in: [Current Contents/Clinical Medicine] [SCI Expanded] [ISI Alerting System] [ISI Journals Master List] [Index Medicus/MEDLINE] [EMBASE/Excerpta Medica] [Chemical Abstracts/CAS]

Table 2 continued. Results from the region of interest-based analysis of fractional anisotropy values of the patient and control groups.

	Patient group	Control group	Difference	p-Value
Fornix (column and body)	0.30±0.08	0.35±0.08	0.05	0.174
Right posterior thalamic radiation (include optic radiation)	0.49±0.05	0.52±0.03	0.03	0.174
Right sagittal stratum (include inferior longitudinal fasciculus and inferior fronto-occipital fasciculus)	0.44±0.03	0.46±0.03	0.02	0.174
Left posterior thalamic radiation (include optic radiation)	0.49±0.04	0.51±0.02	0.02	0.174
Right uncinate fasciculus	0.41±0.04	0.43±0.02	0.02	0.174
Right superior longitudinal fasciculus	0.40±0.02	0.41±0.01	0.01	0.174
Right fornix (crus)	0.39±0.05	0.41±0.04	0.02	0.257
Left tapetum	0.26±0.02	0.27±0.02	0.01	0.257
Left retrolenticular part of internal capsule	0.49±0.02	0.50±0.02	0.01	0.290
Left medial lemniscus	0.52±0.02	0.54±0.03	0.02	0.364
Right retrolenticular part of internal capsule	0.50±0.01	0.50±0.02	0.00	0.545
Left Inferior cerebellar peduncle	0.40±0.02	0.40±0.03	0.00	0.545
Right Inferior cerebellar peduncle	0.40±0.02	0.40±0.03	0.00	0.762

Values represent mean±standard deviation; * significant difference between the patient and control groups, $p<0.05$.

the lowest *P* value. The FA values of the patient group were significantly lower ($P<0.05$) than those of the control group in 19 of the 48 ROIs: the corpus callosum [splenium ($P=0.002$), genu ($P=0.019$), body ($P=0.028$)], both posterior limbs of the internal capsule (right: $P=0.003$; left: $P=0.023$), both corticospinal tracts (right: $P=0.004$; left: $P=0.023$), both superior corona radiata (right: $P=0.016$; left: $P=0.008$), both superior cerebellar peduncles (right: $p=0.041$; left: $P=0.041$), the middle cerebellar peduncle ($P=0.028$), the left anterior limb of the internal capsule ($P=0.028$), the left external capsule ($P=0.028$), the right cingulum (hippocampus, $P=0.028$), the left superior longitudinal fasciculus ($P=0.034$), the left cingulum (cingulate gyrus, $P=0.049$), the left cerebral peduncle ($P=0.007$), and the right posterior corona radiata ($P=0.016$) (**Figure 1**). However, the FA values for the other 29 ROIs showed no significant differences between the patient and control groups ($P>0.05$).

Discussion

The current study investigated microstructural differences in the subcortical white matter of the patient and control groups and obtained the following results: 1) FA values of the patient group were lower than those of the control group in 19 of the 48 white matter ROIs; 2) the ROIs with the lowest ratios for the FA values between the patient and control groups were associated with the corpus callosum and its adjacent neural structures (the corpus callosum and the cingulum), the brainstem and its adjacent neural structures (the cerebral peduncle, the superior and middle cerebellar peduncle), the subcortical white matter that passes the long neural tracts (the internal capsule, the corona radiata, the corticospinal tract, the external capsule, and the superior longitudinal fasciculus).

The FA value, which reflects the grade of water diffusion's directionality and represents the integrity of white matter (eg, indicative of axon diameter, fiber density, and myelination), used to assess white matter status [24-26]. A reduced FA value indicates decreased microstructural integrity of the neural structure of interest [24-26]. Our results show that 19 of the assessed 48 ROIs in the patient group had lower mean FA values than those of the control group, suggesting the existence of neural injuries in these 19 white matter areas. In addition, the 19 ROIs (the corpus callosum, the cingulum, the superior cerebellar peduncle, the middle cerebellar peduncle, the cerebral peduncle, the internal capsule, the corona radiata, the corticospinal tract, the external capsule, and the superior longitudinal fasciculus) showing significant differences between the patient and control groups are consistent with the brain areas vulnerable to DAI [40-42]. DAI can be reflective of a widespread traumatic injury such as that associated with fast acceleration – deceleration of the head in which

Indexed in: [Current Contents/Clinical Medicine] [SCI Expanded] [ISI Alerting System] [ISI Journals Master List] [Index Medicus/MEDLINE] [EMBASE/Excerpta Medica] [Chemical Abstracts/CAS]

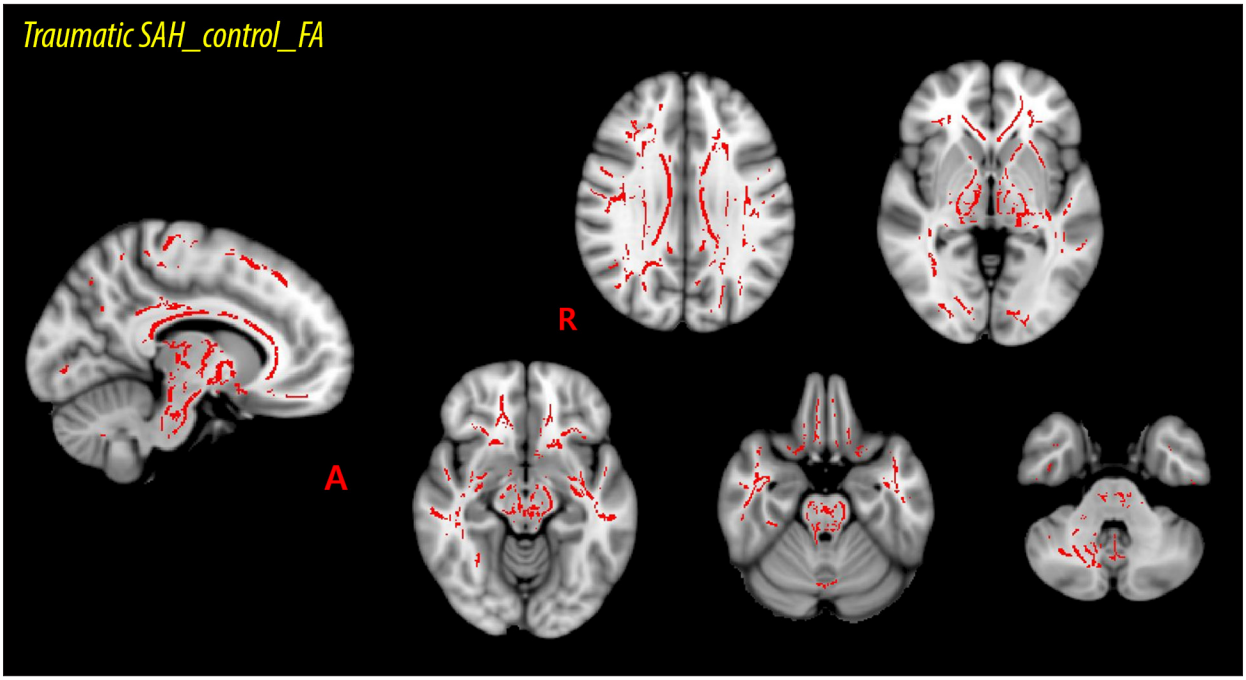

Figure 1. Results of tract-based spatial statics analysis comparing fractional anisotropy (FA) values between the patient and control groups. FA values are acquired for 48 regions of interest (ROIs) applying the white matter atlases standard template of Johns Hopkins University through the Functional Magnetic Resonance Imaging of the Brain Software Library (FSL version 5.1). The red voxels represent areas where the mean FA values are significantly higher in the control group than in the patient group. The FA values of 19 of 48 ROIs (splenium, genu, and body of the corpus callosum, both posterior limbs of the internal capsule, both corticospinal tracts, both superior corona radiata, both superior cerebellar peduncles, the middle cerebellar peduncle, the left anterior limb of the internal capsule, the left external capsule, the right cingulum, the left superior longitudinal fasciculus, the left cingulum, the left cerebral peduncle, the right posterior corona radiata) in the control group are higher than those of the patient group.

the shearing forces lead to mechanical axonal damage [40]. Many previous studies have reported that the common locations for DAI are the corpus callosum (especially the splenium), the subcortical white matter, and the brainstem [40-42]. In addition, injuries to several neural tracts, such as the cingulum, the corticospinal tract, the cerebellar peduncle, the superior and inferior longitudinal fasciculus, and the fornix, have also been detected in DAI patients by using DTT [15-23]. DAI is the chief cause of morbidity and mortality in traumatic brain injury patients [40]. Such patients frequently fall into a coma from the collision time, and survivors usually have severe disabilities. Based on our results, traumatic SAH patients appear to be accompanied by DAI; thus, traumatic SAH could be an indicator of the presence of severe brain injuries related to acute or excessive mechanical forces.

By using DTI, many studies have reported SAH-related neural tract injuries [36,43-55]. However, few studies have assessed the influence of SAH on the entire brain white matter, and recently, Jang et al (2020), by applying TBSS, demonstrated that spontaneous SAH following aneurysmal rupture can induce abnormalities in extensive areas of the subcortical white matter [36]. However, the majority of these previous studies are related to spontaneous aneurysmal SAH, and little has been reported on the neural injuries associated with traumatic SAH. Traumatic SAH is often caused by rupturing of the bridging veins or pial vessels that pass under the subarachnoid membrane or by blood outflow into the subarachnoid space from an adjacent cerebral contusion, rather than via the tear of an aneurysm [56]. Therefore, traumatic SAH would have different clinical symptoms and signs from those of spontaneous aneurysmal SAH, in which previous studies have suggested the symptoms are associated with the location of the hemorrhage, the amount of bleeding, the frequency of vasospasm, and the change in cerebral blood flow [57-59]. Our study also showed that the white matter injury caused by traumatic SAH differs that from the widespread white matter injuries caused by aneurysmal SAH, and the traumatic SAH-related injuries were consistent with those reported in previous studies related to DAI. Further studies on the characteristics of neural injuries of traumatic SAH, which are different from those of spontaneous SAH, should be undertaken.

Many previous studies have used TBSS to identify the abnormalities of white matter in traumatic brain injuries patients, and most of those traumatic injuries were accompanied by

Indexed in: [Current Contents/Clinical Medicine] [SCI Expanded] [ISI Alerting System] [ISI Journals Master List] [Index Medicus/MEDLINE] [EMBASE/Excerpta Medica] [Chemical Abstracts/CAS]

focal axonal injury or DAI [28-35]. In 2009, Perlbarg et al used TBSS to investigate white matter differences between 30 severe traumatic brain injury patients and 10 healthy controls, and observed FA value decrements in the inferior longitudinal fasciculus, the cerebral peduncle, the posterior limb of the internal capsule, and the posterior corpus callosum in the patient group [28]. In 2012, Messé et al compared structural integrity in 53 mild traumatic brain injury patients with that in 40 healthy controls and reported that the patient group had lower FA values than the control group in extensive brain regions, but primarily including the corpus callosum, the cerebellar peduncle, the internal and external capsules, the corona radiata and the thalamic radiation, the sagittal stratum, the fornix, and the superior longitudinal fasciculus [29]. In 2014, Xiong et al compared FA and mean diffusivity (MD) values of 20 mild traumatic brain injury patients with those of 25 healthy control subjects, and reported FA value decrements or MD value increments in the patient group in the uncinate fasciculus, the superior longitudinal fasciculus, the inferior longitudinal fasciculus, the internal capsule, and the corpus callosum [30]. In 2019, Choi et al compared white matter characteristics' differences between 22 DAI patients and 30 healthy controls, and observed extensive diminution of the explicit myelin water fraction in DAI patients [31]. In 2020, Wright et al investigated white matter' differences between 11 retired professional rugby league players with histories of sport-related concussion and 12 healthy controls, and reported FA value decrements or MD value increments in the superior longitudinal fasciculus, the corticospinal tract, the corpus callosum, and the uncinate fasciculus [32]. Furthermore, several other studies have also reported extended abnormalities of the white matter in traumatic brain injury patients contrasted to the white matter of the normal control group [33-35]. Aside from those studies, this is the first TBSS study to prove the abnormalities of white matter in isolated traumatic SAH patients.

Nonetheless, some limitations of our study should be considered. First, the small number of subjects in the study is a limitation. In addition, we could not acquire relevant clinical data because this study was conducted retrospectively. Hence, further prospective studies that include a massive number of subjects and collect more related clinical data are warranted. Second, TBSS collapses white matter tracts into a skeleton framework to mark the middle of the tract and merely projects the highest FA value acquired following the projection to that center; such an approach results in damage of information and the possibility of including data artifacts [60,61]. Third, TBSS methods automatically calculate the skeleton voxels' statistics compared to the less-relevant voxels; thus, family-wise error correction is less punitive [61].

Conclusions

In conclusion, by applying a TBSS, we demonstrated white matter abnormalities in traumatic SAH patients. The corpus callosum and its adjacent neural structures, the brainstem and its adjacent neural structures, and the subcortical white matter that passes the long neural tracts were shown to have neural injuries in traumatic SAH patients, and these results are consistent with brain areas vulnerable to DAI. Therefore, traumatic SAH patients appeared to be accompanied by DAI, and traumatic SAH could be an indicator of the presence of severe brain injuries related to acute or excessive mechanical forces. Furthermore, we believe our results will be useful in future studies aimed at clarifying the pathophysiology of brain injury in traumatic SAH.

Declaration of Figures Authenticity

All figures submitted have been created by the authors, who confirm that the images are original with no duplication and have not been previously published in whole or in part.

References:

1. Abraham MK, Chang WW. Subarachnoid hemorrhage. Emerg Med Clin N Am. 2016;34:901-16
2. Zacko JC, Haris L, Bullock MR. Surgical management of traumatic brain injury. In: Richard Winn H, editor. Youmans Neurological Surgery. 6th ed. Ch. 335. Philadelphia: Saunders, 2011;3428
3. Eisenberg HM, Gary HE, Aldrich EF, et al. Initial CT findings in 753 patients with severe head injury: A report from the NIH Traumatic Coma Data Bank. J Neurosurg. 1990;73:688-98
4. Murray GD, Teasdale GM, Braakman R, et al. The European brain injury consortium survey of head injuries. Acta Neurochir (Wien). 1999;141:223-36
5. Kakarieka A. Traumatic subarachnoid haemorrhage. Berlin: Springer, 1997;1-109
6. Green KA, Marciano FF, Johnson BA, et al. Impact of traumatic subarachnoid hemorrhage on outcome in nonpenetrating head injury. J Neurosurg. 1995;83:445-52
7. Servadei F, Murray GD, Teasdale GM, et al. Traumatic subarachnoid hemorrhage: Demographic and clinical Study of 750 patients from the European brain injury consortium survey of head injuries. Neurosurgery. 2002;50:261-69
8. Lee JH, Martin NA, Alsina G, et al. Hemodynamically significant cerebral vasospasm and outcome after head injury: A prospective study. J Neurosurg. 1997;87:221-33
9. Chestnut RM, Luerssen TG. Post-traumatic ventricular enlargement in the Traumatic Coma Data Bank: Incidence, risk factors, and influence on outcome. Presented at proceedings of the 8th international symposium on intracranial pressure. Berlin: Springer-Verlag, 1993;503-6
10. Grcevic N. Traumatic tears of the tela chorioidea: A hitherto unrecognized cause of post-traumatic hydrocephalus. Acta Neurochir Suppl (Wien). 1983;32:79-85
11. Sarkari A, Gupta DK, Sinha S, et al. Post-traumatic hydrocephalus: Presentation, management and outcome-an apex trauma centre experience. Indian J Neurotrauma. 2010;7:135-38
12. Tian HL, Xu T, Hu J, et al. Risk factors related to hydrocephalus after traumatic subarachnoid hemorrhage. Surg Neurol. 2008;69:241-46

Indexed in: [Current Contents/Clinical Medicine] [SCI Expanded] [ISI Alerting System] [ISI Journals Master List] [Index Medicus/MEDLINE] [EMBASE/Excerpta Medica] [Chemical Abstracts/CAS]

13. Aminmansour B, Ghorbani A, Sharifi D, et al. Cerebral vasospasm following traumatic subarachnoid hemorrhage. J Res Med Sci. 2009;14:343-48
14. Javed Z, Qamar U, Sathyapalan T. Pituitary and/or hypothalamic dysfunction following moderate to severe traumatic brain injury: Current perspectives. Indian J Endocrinol Metab. 2015;19:753-63
15. Kwon HG, Jang SH. The usefulness of diffusion tensor imaging in detection of diffuse axonal injury in a patient with head trauma. Neural Regen Res. 2012;7:475-78
16. Jang SH, Kim OL, Kim SH, Lee HD. Differences in corpus callosum injury between cerebral concussion and diffuse axonal injury. Medicine (Baltimore). 2019;98:e17467
17. Jang SH, Kim SH, Lee HD. Traumatic axonal injury of the cingulum in patients with mild traumatic brain injury: A diffusion tensor tractography study. Neural Regen Res. 2019;14:1556-61
18. Hong JH, Kim OL, Kim SH, et al. Cerebellar peduncle injury in patients with ataxia following diffuse axonal injury. Brain Res Bull. 2009;80:30-35
19. Hong JH, Jang SH. Degeneration of cingulum and fornix in a patient with traumatic brain injury: Diffuse tensor tractography study. J Rehabil Med. 2010;42:979-81
20. Seo JP, Jang SH. Traumatic axonal injury of the corticospinal tract in the subcortical white matter in patients with mild traumatic brain injury. Brain inj. 2015;29:110-14
21. Jang SH. Diffusion tensor imaging studies on corticospinal tract injury following traumatic brain injury: A review. NeuroRehabilitation. 2011;29:339-45
22. Kraus MF, Susmaras T, Caughlin BP, et al. White matter integrity and cognition in chronic traumatic brain injury: A diffusion tensor imaging study. Brain. 2007;130(Pt 10):2508-19
23. Kasahara K, Hashimoto K, Abo M, Senoo A. Voxel- and atlas-based analysis of diffusion tensor imaging may reveal focal axonal injuries in mild traumatic brain injury – comparison with diffuse axonal injury. Magn Reson Imaging. 2012;30:496-505
24. Basser PJ, Mattiello J, LeBihan D. Estimation of the effective self-diffusion tensor from the NMR spin echo. J Magn Reson B. 1994;103:247-54
25. Mori S, Crain BJ, Chacko VP, van Zijl PC. Three-dimensional tracking of axonal projections in the brain by magnetic resonance imaging. Ann Neurol. 1999;45:265-69
26. Alexander AL, Lee JE, Lazar M, Field AS. Diffusion tensor imaging of the brain. Neurotherapeutics. 2007;4:316-29
27. Smith SM, Jenkinson M, Johansen-Berg H, et al. Tract-based spatial statistics: Voxel wise analysis of multi-subject diffusion data. Neuroimage. 2006;31:1487-505
28. Perlbarg V, Puybasset L, Tollard E, et al. Relation between brain lesion location and clinical outcome in patients with severe traumatic brain injury: A diffusion tensor imaging study using voxel-based approaches. Hum Brain Mapp. 2009;30:3924-33
29. Messé A, Caplain S, Paradot G, et al. Diffusion tensor imaging and white matter lesions at the subacute stage in mild traumatic brain injury with persistent neurobehavioral impairment. Hum Brain Mapp. 2011;32:999-1011
30. Xiong K, Zhu Y, Zhang Y, et al. White matter integrity and cognition in mild traumatic brain injury following motor vehicle accident. Brain Res. 2014;1591:86-92
31. Choi JY, Hart T, Whyte J, et al. Myelin water imaging of moderate to severe diffuse traumatic brain injury. Neuroimage Clin. 2019;22:101785
32. Wright DK, Gardner AJ, Wojtowicz M, et al. White matter abnormalities in retired professional rugby league players with a history of concussion. J Neurotrauma. 2021;38:983-88
33. Kinnunen KM, Greenwood R, Powell JH, et al. White matter damage and cognitive impairment after traumatic brain injury. Brain. 2011;134:449-63
34. Yamagata B, Ueda R, Tasato K, et al. Widespread white matter aberrations are associated with phonemic verbal fluency impairment in chronic traumatic brain injury. J Neurotrauma. 2020;37:975-81
35. Chung S, Fieremans E, Wang X, et al. White matter tract integrity: An indicator of axonal pathology after mild traumatic brain injury. J Neurotrauma. 2018;35:1015-20
36. Lee SJ, Kim MS, Jang SH. White matter abnormalities in spontaneous subarachnoid hemorrhage: A tract-based spatial statistics study. Stroke. 2020;51:e246-49
37. Smith SM, Jenkinson M, Woolrich MW, et al. Advances in functional and structural MR image analysis and implementation as FSL. Neuroimage. 2004;23(Suppl.1): S208-19
38. Cho MJ, Jang SH. Relationship between post-traumatic amnesia and white matter integrity in traumatic brain injury using tract-based spatial statistics. Sci Rep. 2021;11:6898
39. Anjari M, Srinivasan L, Allsop JM, et al. Diffusion tensor imaging with tract-based spatial statistics reveals local white matter abnormalities in preterm infants. Neuroimage. 2007;35:1021-27
40. Benson C. Diffuse axonal injury. Encyclopedia of the Neurological Sciences. 2nd ed. Amsterdam: Elsevier, 2014;998-99
41. Adams JH, Doyle D, Ford I, et al. Diffuse axonal injury in head injury: Definition, diagnosis and grading. Histopathology. 1989;15:49-59
42. Meythaler JM, Peduzzi JD, Eleftheriou E, Novack TA. Current concepts: Diffuse axonal injury-associated traumatic brain injury. Arch Phys Med Rehabil. 2001;82:1461-71
43. Hong JH, Choi BY, Chang CH, et al. Injuries of the cingulum and fornix after rupture of an anterior communicating artery aneurysm: A diffusion tensor tractography study. Neurosurgery. 2012;70:819-23
44. Yeo SS, Choi BY, Chang CH, et al. Evidence of corticospinal tract injury at midbrain in patients with subarachnoid hemorrhage. Stroke. 2012;43:2239-41
45. Sener S, Van Hecke W, Feyen BF, et al. Diffusion tensor imaging: A possible biomarker in severe traumatic brain injury and aneurysmal subarachnoid hemorrhage? Neurosurgery. 2016;79:786-93
46. Schweizer TA, Al-Khindi T, Loch Macdonald R. Diffusion tensor imaging as a surrogate marker for outcome after perimesencephalic subarachnoid hemorrhage. Clin Neurol Neurosurg 2012;114:798-800
47. Jang SH, Choi BY, Kim SH, et al. Injury of the mammillothalamic tract in patients with subarachnoid haemorrhage: A retrospective diffusion tensor imaging study. BMJ Open. 2014;4:e005613
48. Jang SH, Choi BY, Kim SH, et al. Injury of the corticoreticular pathway in subarachnoid haemorrhage after rupture of a cerebral artery aneurysm. J Rehabil Med. 2015;47:133-37
49. Jang SH, Kim HS. Aneurysmal subarachnoid hemorrhage causes injury of the ascending reticular activating system: relation to consciousness. Am J Neuroradiol. 2015;36:667-71
50. Jang SH, Yeo SS. Injury of the papez circuit in a patient with provoked confabulation following subarachnoid hemorrhage: A diffusion tensor tractography study. Acta Neurol Belg. 2016;116:655-58
51. Jang SH, Seo JP. Injury of optic radiation and visual field defect in a patient with aneurysmal subarachnoid hemorrhage: A case report. Medicine. 2017;96:e7356
52. Darwazeh R, Wei M, Zhong J, et al. Significant injury of the mammillothalamic tract without injury of the corticospinal tract after aneurysmal subarachnoid hemorrhage: A retrospective diffusion tensor imaging study. World Neurosurg. 2018;114:e624-30
53. Jang SH, Chang CH, Jung YJ, et al. Optic radiation injury in patients with aneurismal subarachnoid hemorrhage: A preliminary diffusion tensor imaging report. Neural Regen Res. 2018;13:563-66
54. Jang SH, Yeo SS. Injury of the precommissural fornix in a patient with subarachnoid hemorrhage: A case report. J Stroke Cerebrovasc Dis. 2018;27:e98-101
55. Reijmer YD, Van den Heerik MS, Heinen R, et al. Microstructural white matter abnormalities and cognitive impairment after aneurysmal subarachnoid hemorrhage. Stroke. 2018;49:2040-45
56. Ullman JS, Morgan BC, Eisenberg HM. Traumatic subarachnoid hemorrhage. Textbook of subarachnoid hemorrhage: Pathophysiology and management. AANS. 1997;225-37
57. Fukuda T, Hasue M, Ito H. Does traumatic subarachnoid hemorrhage caused by diffuse brain injury cause delayed ischemic brain damage? Comparison with subarachnoid hemorrhage caused by ruptured intracranial aneurysm. Neurosurgery. 1998;43:1040-49
58. Gomez CR, Backer RJ, Bucholz RD. Transcranial Doppler ultrasound following closed head injury: Vasospasm or vasoparalysis? Surg Neurol. 1991;35:30-35
59. Sander D, Klingelhofer J. Cerebral vasospasm following post-traumatic subarachnoid hemorrhage evaluated by transcranial Doppler ultrasonography. J Neurol Sci. 1993;119:1-7
60. Zalesky A. Moderating registration misalignment in voxelwise comparisons of DTI data: A performance evaluation of skeleton projection. Magn Reson Imaging. 2011;29:111-25
61. Schwarz CG, Reid RI, Gunter JL, et al. Improved DTI registration allows voxel-based analysis that outperforms tract-based spatial statistics. Neuroimage. 2014;94:65-78

Indexed in: [Current Contents/Clinical Medicine] [SCI Expanded] [ISI Alerting System] [ISI Journals Master List] [Index Medicus/MEDLINE] [EMBASE/Excerpta Medica] [Chemical Abstracts/CAS]